Solid-State NMR Investigation of the Membrane-Disrupting Mechanism of Antimicrobial Peptides MSI-78 and MSI-594 Derived from Magainin 2 and Melittin

Ayyalusamy Ramamoorthy,* Sathiah Thennarasu,* Dong-Kuk Lee,* Anmin Tan,* and Lee Maloy†
*Biophysics Research Division and Department of Chemistry, University of Michigan, Ann Arbor, Michigan 48109-1055; and
†Genaera Pharmaceuticals, Plymouth Meeting, Pennsylvania

ABSTRACT The mechanism of membrane interaction of two amphipathic antimicrobial peptides, MSI-78 and MSI-594, derived from magainin-2 and melittin, is presented. Both the peptides show excellent antimicrobial activity. The 8-anilinonaphthalene-1-sulfonic acid uptake experiment using *Escherichia coli* cells suggests that the outer membrane permeabilization is mainly due to electrostatic interactions. The interaction of MSI-78 and MSI-594 with lipid membranes was studied using ^{31}P and ^{2}H solid-state NMR, circular dichroism, and differential scanning calorimetry techniques. The binding of MSI-78 and MSI-594 to the lipid membrane is associated with a random coil to α-helix structural transition. MSI-78 and MSI-594 also induce the release of entrapped dye from POPC/POPG (3:1) vesicles. Measurement of the phase-transition temperature of peptide-DiPoPE dispersions shows that both MSI-78 and MSI-594 repress the lamellar-to-inverted hexagonal phase transition by inducing positive curvature strain. ^{15}N NMR data suggest that both the peptides are oriented nearly perpendicular to the bilayer normal, which infers that the peptides most likely do not function via a barrel-stave mechanism of membrane-disruption. Data obtained from ^{31}P NMR measurements using peptide-incorporated POPC and POPG oriented lamellar bilayers show a disorder in the orientation of lipids up to a peptide/lipid ratio of 1:20, and the formation of nonbilayer structures at peptide/lipid ratio $>$1:8. ^{2}H-NMR experiments with selectively deuterated lipids reveal peptide-induced disorder in the methylene units of the lipid acyl chains. These results are discussed in light of lipid-peptide interactions leading to the disruption of membrane via either a carpet or a toroidal-type mechanism.

INTRODUCTION

Linear and cyclic antimicrobial peptides are produced as a part of the host defense mechanisms by various organisms that include microbes, insects, plants, vertebrates, and mammals (1). A large number of antimicrobial peptides are cationic and display molecular amphipathicity despite their structural diversity (2,3). Unlike conventional antibiotics that bind to a target in the membrane or cytosol, most antimicrobial peptides kill cells by permeabilizing the cell membrane through peptide-lipid interactions (4,5). Various mechanisms have been proposed for killing bacteria. These include the formation of discrete channels that dissipate ion gradients across the membrane (6,7), disturbance of the lipid bilayer as a result of carpet-like peptide binding (8), phase separation due to specific peptide-lipid interactions (9), and detergent-like solubilization of the membrane (10). In recent years, pathogenic microorganisms have increasingly developed resistance to conventional antibiotics (11). Since the development of resistance to membrane-active peptides appears to be very rare (12), there is a considerable interest in developing antimicrobial peptides for pharmaceutical applications (13).

Several attempts have been made to design peptides with improved antimicrobial activity and low toxicity (14). They include 1), structure activity relationship of natural peptides; 2), chemical modifications such as cyclization, linearization, and fatty acylation of antimicrobial peptides; 3), de novo design of amphipathic model peptides; and 4), synthetic peptide hybrids. The design of peptides that selectively interact with biological membranes has taken into consideration the various physicochemical properties such as the net charge (13), hydrophobic moment (15), helical content (16,17), and the angle subtended by the polar/apolar faces (18). An increase in hydrophobicity has been shown to increase the hemolytic activity (13,19). However, the exact attributes of these physicochemical properties are still unclear.

Submitted September 11, 2005, and accepted for publication March 14, 2006.

Address reprint requests to Dr. A. Ramamoorthy, Biophysics Research Division and Dept. of Chemistry, University of Michigan, Ann Arbor, MI 48109-1055. Tel.: 734-647-6572; Fax: 734-763-2307; E-mail: ramamoor@umich.edu.

Sathia Thennarasu's present address is Organic Chemistry Division, Central Leather Research Institute, Chennai 600020, India.

Dong-Kuk Lee's present address is Dept. of Fine Chemistry, Seoul National University of Technology, Seoul, Korea 139-743.

Abbreviations used: ANS, 8-anilinonapthalene-1-sulfonic acid; CD, circular dichroism; DSC, differential scanning calorimetry; DiPoPE, 1,2-dipalmitoleoyl-*sn*-glycero-3-phosphatidylethanolamine; H_I, normal hexagonal phase; H_{II}, inverted hexagonal phase; L_α, fluid lamellar phase; MIC, minimal inhibitory concentration; MLV, multilamellar vesicle; NMR, nuclear magnetic resonance; PISEMA, polarization inversion spin exchange at the magic angle; POPC, 1-palmitoyl-2-oleoyl-*sn*-glycero-3-phosphatidylcholine; POPC-d_{31}, 1-d_{31}-palmitoyl-2-oleoyl-*sn*-glycero-3-phosphatidylcholine; POPG, 1-palmitoyl-2-oleoyl-*sn*-glycero-3-phosphatidylglycerol; σ_{para}, parallel edge of the ^{31}P chemical shift powder pattern; σ_{perp}, perpendicular edge of the ^{31}P chemical shift powder pattern; $\sigma_{para} - \sigma_{perp}$, span of chemical shift anisotropy; P/L, peptide/lipid molar ratio; SUV, small unilamellar vesicle.

0006-3495/06/07/206/11 $2.00

doi: 10.1529/biophysj.105.073890

A series of peptides based on the naturally isolated magainin (magainin2 and PGLa) have been designed for potential pharmaceutical applications. Among these peptides, MSI-78 and MSI-594 show more potent antimicrobial activities than magainin2 (Tables 1 and 2). MSI-78 is an analog of magainin 2, which was first isolated from the frog *Xenopus laevis* (20). MSI-594 is a hybrid of MSI-78 (residues 1 to 11) and melittin (residues 1 to 13), the bee venom toxin (21). Our previous NMR and DSC studies on MSI-78 reported the induction of positive curvature strain on lipid bilayers and the formation of toroidal-type disruption of bilayers (22). Our recent AFM and NMR studies reported the MSI-78-induced bilayer thinning effects (23). On the other hand, there are no biophysical studies so far reported on MSI-594. In this study, we address four questions: Does the helicity of peptides correlate with their membrane permeabilizing ability? Do changes in net charge and hydrophobicity affect the antimicrobial activity and microbial membrane disrupting ability? What is the location of MSI-78 and MSI-594 in lipid bilayers? How do they disrupt membranes, by the formation of pores or the carpet mechanism? Fluorescence studies on MSI-78 are reported here for the first time, and NMR results on MSI-78 are discussed along with previous studies on this peptide. These results are also helpful for understanding the biophysical properties of these two related peptides.

The antimicrobial susceptibility assay shows that the activities of both MSI-78 and MSI-594 against Gram-positive and Gram-negative bacteria are comparable. However, they differ in their ability to disrupt the bacterial cell wall, as observed in the ANS uptake assay. Circular dichroism experiments reveal that both MSI-78 and MSI-594 are unordered in aqueous medium but fold into helical conformation with varying helical content in a lipid environment. However, the ability of these two peptides to permeabilize negatively charged liposomes mimicking bacterial inner membrane are comparable, as evidenced from the dye leakage experiment. ^{15}N NMR data suggest that both the peptides are oriented nearly perpendicular to the bilayer normal. ^{31}P NMR spectra of peptide-incorporated lipid bilayers show that both peptides bind in the phosphate headgroup region of POPC and POPG bilayers and perturb the lamellar-phase lipid bilayer structures at a higher concentration. Order parameters determined from de-Paked ^{2}H NMR spectra of selectively labeled POPC-d_{31} MLVs incorporated with MSI-78 and MSI-594, indicate a disordering effect in the hydrocarbon chain. Differential scanning calorimetry shows that the L_α-to-H_{II} phase transition temperature increases when MSI-78 or MSI-594 is incorporated into DiPoPE bilayers. The influence of subtle variations in helicity, hydrophobicity, and net charge of these peptides on the lipid-peptide interactions is discussed.

TABLE 2 MIC values of magainin analogs against microorganisms

Strain	Magainin-2*	MSI-78	MSI-594
E. coli	10	4	2
Staphyloccus aureus	50–75	4	4
Pseudomonas aeruginosa	70–100	4	4
C. albicans	25	64	64

All values given are in μg.
*MIC values for magainin-2 were taken from the literature (13).

MATERIALS AND METHODS

POPG, POPC, POPC-d_{31}, and DiPoPE were purchased from Avanti Polar Lipids (Alabaster, AL). Chloroform and methanol were procured from Aldrich Chemical (Milwaukee, WI). Naphthalene was purchased from Fisher Scientific (Pittsburgh, PA). Peptide synthesis and cleavage reagents were purchased from Applied Biosystems (Foster City, CA) and Aldrich (Milwaukee, WI), respectively. Fmoc-protected amino acids were from Advanced ChemTech (Louisville, KY), and isotopically labeled Fmoc-amino acids were from Cambridge Isotope Labs (Cambridge, MA). All the chemicals were used without further purification. The unlabeled peptides were synthesized by Genaera Corp. (Plymouth Meeting, PA). ^{15}N-Phe$_{16}$-labeled MSI-78 was synthesized and purified at the University of Michigan, as explained elsewhere (13).

Antimicrobial assay

A doubling dilution series of peptide, beginning with 100 μg/mL, was added to the wells of a sterile 384-well microtiter plate (12 replicates per dilution) and dried overnight in a desiccator box. Bacterial suspensions (10 μL, 10^7/mL) were added to the wells, covered with a sterile plastic film, centrifuged briefly to collect the cells in the bottom of the wells, and incubated at 37°C for 6–36 h, depending upon the rate of growth of the bacterial species. Bacteria were incubated in normal atmosphere. The terminal cell numbers were determined by turbidometric method ($OD_{600} = 0.02$). MICs were set as the lowest concentration of the peptide at which there was no growth above the inoculated level of bacteria ($p < 0.05$, $n = 12$). Values expressed in the tables represent Log_{10} growth above inoculated levels.

Outer membrane disruption assay

The outer membrane permeabilizing ability was investigated using the ANS uptake assay (24), using *Escherichia coli* strain BL21 (DE3). Bacterial cells from an overnight culture were inoculated into LB medium. Cells from the mid-log phase were centrifuged and washed with buffer (10 mM Tris, 150 mM NaCl, pH 7.4), and then resuspended in the same buffer to an OD_{600} of 1.2. To 3.0 mL of the cell suspension in a cuvette, a stock solution of ANS was added to a final concentration of 5.0 μM. The degree of membrane disruption as a function of peptide concentration was observed by the increase in fluorescence intensity at ~500 nm.

TABLE 1 Physical parameters of magainin analogs

Peptide	Amino acid sequence	Net cationic charge	GRAVY	Aliphatic index	Hydrophobic moment
MSI-78	GIGKFLKKAKKFGKAFVKILKK-NH2	9	−0.159	93.18	0.65
MSI-594	GIGKFLKKAKKGIGAVLKVLTTGL-NH2	6	0.508	130.00	0.59

Dye leakage assay

Carboxyfluorescein dye entrapped SUVs were prepared as described elsewhere (24). The dye-containing vesicles were then purified by gel filtration chromatography, using a Sephadex G-75 column. Aliquots of peptide solution were added to a stirred suspension of SUVs and the fluorescence emission intensity as a function of time was recorded using the excitation wavelength 490 nm and the emission wavelength 520 nm. The maximum leakage from each sample was determined by adding 1% TritonX-100.

Circular dichroism

SUVs were prepared by suspending dry POPC in Tris buffer (10 mM Tris·HCl, 100 mM NaCl, 0.1 mM EDTA, pH 7.4) and sonicating the dispersion until a clear solution was obtained. 40 μM peptide stock solutions were also prepared using Tris buffer. Each sample was prepared as a 1:1 (vol/vol) mixture of peptide and lipid SUV stock solutions with additional Tris buffer as needed in a 5-mm quartz cuvette. The sample was then equilibrated to 25°C in the CD spectrometer (AVIV, Lakewood, NJ) for 10 min and five scans were acquired and averaged. The scan rate was 1 nm/min over the range 190–280 nm. Background contributions from the buffer and SUVs were removed by subtracting the spectrum of a similar sample without peptide. The mean helix content, f_H, was determined from the ellipticity value at λ_{222} nm, $[\Theta]_{222}$, using the empirical equation given below (25):

$$f_H = ([\Theta]_{222} - \Theta_C)/(\Theta_H - \Theta_C);$$

where Θ_C and Θ_H are given as:

$$\Theta_C = 2220 - 53T;$$
$$\Theta_H = (-44000 + 250T)(1 - 3/N_r),$$

where T is the temperature in degrees Celsius and N_r is the number of residues in the peptide.

Differential scanning calorimetry

Samples were prepared by codissolving the peptides and DiPoPE in a 2:1 $CHCl_3/CH_3OH$ solution. The solution was dried under a stream of nitrogen and then under high vacuum for several hours. Buffer (10 mM Tris-HCl, 100 mM NaCl, 2 mM EDTA, pH 7.4) was added to each sample and vortexed to resuspend the peptide and lipid; the final concentration was 10 mg/ml lipid solution. The solutions were degassed under vacuum for 15 min before DSC measurements. The heating scan rate was 1°C/min. The L_α-to-H_{II} transition temperature of the lipids was measured on a CSC 6100 Nano II Differential Scanning Calorimeter (Calorimetry Sciences, Provo, UT). The raw data were then converted to molar heat capacity using the CPCalc program available with the calorimeter. In each conversion, the average lipid molecular weight for each sample and a partial specific volume of 0.956 mL/g were used.

Solid-state NMR

All mechanically aligned lipid samples were prepared using the naphthalene procedure (26). Briefly, 4 mg of lipids and an appropriate amount of peptide were dissolved in an excess of 2:1 $CHCl_3/CH_3OH$. The lipid-peptide solution was dried under a stream of N_2 gas and redissolved in 2:1 $CHCl_3/CH_3OH$ containing a 1:1 molar ratio of naphthalene to lipid-peptide. The solution was then dried on two thin glass plates (11 mm × 22 mm × 50 μm, Paul Marienfeld GmbH & Co., Bad Mergentheim, Germany). To remove the naphthalene and any residual organic solvents, the samples were dried under vacuum for at least 10 h. After drying, the samples were indirectly hydrated in a hydration chamber at 93% relative humidity using a saturated $NH_4H_2PO_4$ solution (27) for 2–3 days at 37°C, after which ~2 μL of H_2O was misted onto the surface of the lipid-peptide film on the glass plates. The glass plates were then stacked, wrapped using parafilm, sealed in plastic bags (Plastic Bagmart, Marietta, GA), and further equilibrated at 4°C for 6–24 h. MLVs were prepared by mixing 5 mg lipid and the desired amount of peptide in 2:1 $CHCl_3/CH_3OH$, but no naphthalene was used. The samples were dried under N_2 and vacuum-dried overnight. Pure water (deuterium-depleted water for ^2H NMR samples) was added and the sample was gently vortexed, followed by several freeze-thaw cycles to produce MLVs.

All of the experiments were performed on a Chemagnetics/Varian (Fort Collins, CO) Infinity 400 MHz solid-state NMR spectrometer operating at resonance frequencies of 400.138, 161.979, 61.424, and 40.55 MHz for ^1H, ^{31}P, ^2H, and ^{15}N nuclei, respectively. Unless otherwise noted, all experiments were performed at 30°C. A Chemagnetics/Varian temperature controller unit was used to maintain the sample temperature, and each sample was equilibrated for at least 30 min before starting the experiment. All experiments on oriented samples were performed with the bilayer normal parallel to the external magnetic field. The ^{31}P and ^{15}N chemical shift spectra of mechanically aligned samples were obtained using a home-built double resonance probe. The ^{15}N spectrum of labeled peptide in oriented bilayers was acquired using a ramp cross-polarization sequence with a ^1H $\pi/2$ pulse length of 3.5 μs, 35 kHz cross-polarization power, and a ^1H decoupling of 71 kHz during acquisition. The recycle delay was 3 s and the spectral width was 50 kHz. A 1.25 ms ramp CP with a 10-kHz ramp on the ^1H channel was used. ^{31}P and ^2H powder spectra of MLVs were obtained using a Chemagnetics double resonance probe. A typical ^{31}P 90°-pulse length of 3.1 μs was used in both probes. ^{31}P spectra were obtained using a spin-echo sequence (90°-τ-180°-τ-acq with $\tau = 100$ μs), 40 kHz proton-decoupling rf field, 50 kHz spectral width, and a recycle delay of ~4 s. A typical spectrum required the coaddition of 100–1000 transients. The ^{31}P chemical shift spectra are referenced relative to 85% H_3PO_4 on thin glass plates (0 ppm). ^2H quadrupole coupling spectra were obtained using a quadrupole-echo sequence (90°-τ-90°-τ-acq with $\tau = 60$ μs, with a 90°-pulse length of 3.0 μs, a spectral width of 100 kHz, and a recycle delay of 2 s. A typical ^2H spectrum required the coaddition of 15,000-20,000 transients. All experimental data were processed using the Spinsight (Chemagnetics/Varian) software on a Sun Sparc workstation. De-paking of the ^2H spectra of the POPC-d_{31} MLVs was done on a PC using MATLAB (28,29).

Spectra of MLVs and oriented bilayers

In fully hydrated lipid bilayers, the lipid molecules rotate rapidly around the long molecular axis, and therefore the ^{31}P chemical shift powder spectrum is axially symmetric (30). The discontinuity at the high-frequency side is referred to as the parallel edge (σ_{para}), since it corresponds to the chemical shift value with the lipid rotation axis parallel to the external magnetic field. The discontinuity at the low-frequency side is referred to as the perpendicular edge (σ_{perp}) because it corresponds to the orientation of lipid molecules whose rotation axis is perpendicular to the external magnetic field. For a well-oriented sample with the bilayer normal parallel to the external magnetic field, a single peak would be observed close to σ_{para}. When a lipid molecule in the oriented sample is tilted, the peak in the ^{31}P spectrum occurs at a frequency, ν_{obs}:

$$\nu_{obs} = (\sigma_{para} - \sigma_{perp})\cos^2\theta + \sigma_{perp},$$

where θ is the angle between the axis of lipid rotation and the external magnetic field direction. σ_{para} and σ_{perp} are determined from a spectrum of MLVs.

RESULTS

The amino acid sequences of MSI-78 and MSI-594 are given in Table 1. These two peptides differ in net charge and

hydrophobicity. The aliphatic index, hydrophobicity and hydrophobic moment values were calculated as described elsewhere (31,32). The helical wheel projections of the peptides (Fig. 1) show that the hydrophobic/polar angle subtended by the α-helix is 180°. The underlying assumption is that all residues are involved in helix formation.

Antimicrobial activity and cell wall disruption

The MIC values of MSI-78 and MSI-594 against different bacteria were determined and compared with that of magainin-2. Both MSI-78 and MSI-594 exhibit potent activity against bacteria and fungus. These peptides are more active against bacteria and less active against *Candida albicans* than magainin 2 (Table 2). To understand the mechanism of killing of bacteria, the efficacy of these peptides to disrupt the outer membrane of *E. coli* was assayed using ANS dye. The fluorescence of ANS is dynamically quenched by the polar water molecules and significantly enhanced in the hydrophobic milieu of cell membranes. Disruption of the outer membrane integrity by membrane-active peptides results in the entry of dye into the perturbed membrane, where it emits more intense fluorescence (24). When *E. coli* cells pre-equilibrated with ANS dye were incubated with serial concentrations of MSI-78 or MSI-594, dose-dependent changes in the steady-state fluorescence spectrum of ANS (Fig. 2, *A* and *B*) were observed. Fluorescence spectra were recorded after incubating the cells for ~5 min which allowed maximal ANS uptake (data not shown). The control experiment in which *E. coli* cells were incubated with ANS dye (without peptides) showed no time-dependent changes in the fluorescence spectrum. The dose-dependent maximal fluorescence intensity (Fig. 2 *A*) and the associated blue shift in the emission maximum (Fig. 2 *B*) could be described to the ANS uptake satisfactorily. Interestingly, the data in Fig. 2 *B* suggest that MSI-594, which is more hydrophobic than MSI-78, is weaker than MSI-78 in cell-wall disruption.

Because MSI-78 and MSI-594 showed differential membrane disruption effect despite the fact that their MIC values were comparable, the ability of these peptides to permeabilize model membranes mimicking the bacterial inner membrane was examined. Peptide induced leakage of carboxyfluorescein dye from negatively charged POPC/POPG (3:1) lipid vesicles is shown in Fig. 3 *A* and the percentage of dye release in 5 min is given in Fig. 3 *B*. Dye leakage from POPC/POPG (3:1) vesicles was observed even at a P/L ratio of 1:1000. It is apparent from Fig. 3 that both MSI-78 and MSI-594 are capable of permeabilizing bacterial inner membrane at comparable concentrations.

Secondary structure

The CD spectra of MSI-78 and MSI-594 in buffer and in the presence of POPC SUVs at 25°C are given in Fig. 4. Both MSI-78 and MSI-594 exist as random coils in aqueous medium (Fig. 4 *A*) and fold into predominantly α-helical conformation upon binding to lipid vesicles (Fig. 4 *B*). The CD spectra of vesicle-bound peptides are characterized by the double minima at 208 and 222 nm, attributable to helical conformation. The peptides are assumed to be completely bound to the lipid vesicles at the lipid/peptide ratio of 200:1 used in the study presented here, as the spectra do not change upon increasing the lipid/peptide ratio (33). The mean helix contents of vesicle-bound MSI-78 and MSI-594, as calculated from the mean residue ellipticity values at λ_{222} nm (25), are 40% and 50%, respectively.

Orientation of MSI-78 and MSI-594 in bilayers

The orientations of MSI-78 and MSI-594 in phospholipid bilayers were determined using solid-state NMR experiments on mechanically aligned bilayers containing various concentrations of peptides labeled with ^{15}N at a single site. The alignment of these samples was confirmed by recording ^{31}P chemical shift spectra. All aligned ^{15}N spectra showed a single narrow peak suggesting that the embedded peptides were aligned in bilayers; some sample spectra are shown in Fig. 5. The ^{15}N chemical shift values were measured and given in Table 3. Proton-decoupled ^{15}N chemical shift spectra of mechanically aligned bilayer samples containing ^{15}N-Phe$_{16}$-labeled MSI-78 are given in Fig. 5 *A*. These spectra contain a single peak in a frequency region that corresponds to the perpendicular edge of an unaligned ^{15}N chemical shift anisotropy spectrum. The chemical shift value and the line width slightly change with the lipid composition and concentration of the peptide in bilayers (Table 3). For example, the value is 86 ppm in POPC and 81 ppm in 3:1 POPC/POPG

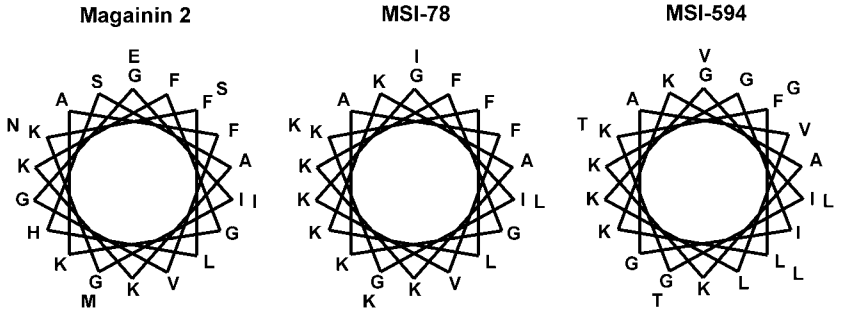

FIGURE 1 Helical wheel representations of magainin 2 (*left*), MSI-78 (*middle*), and MSI-594 (*right*). When all the residues are assumed to be part of the helix, the hydrophobic angle for MSI-78 and MSI-594 is 180°.

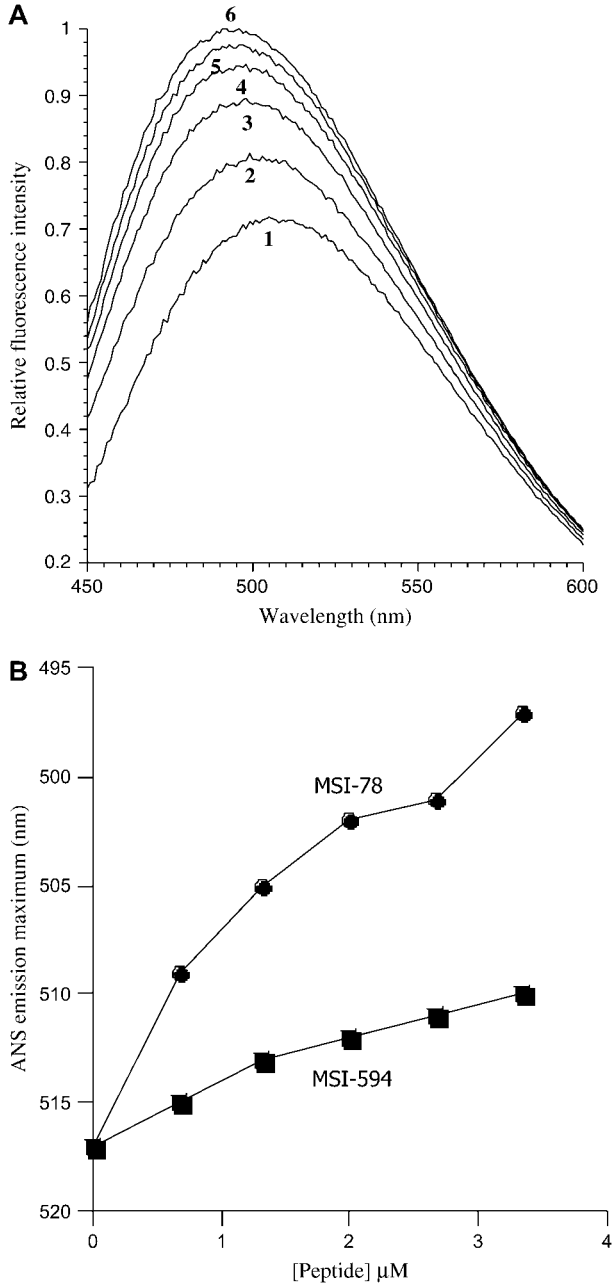

FIGURE 2 (*A*) MSI-78-induced ANS uptake into *E. coli* membrane. Fluorescence spectrum of ANS equilibrated with *E. coli* cells (*1*), and in the presence of 0.67 μM (*2*), 1.33 μM (*3*), 2.0 μM (*4*) and 2.67 μM (*5*), and 3.35 μM (*6*) concentrations of MSI-78. The *E. coli* cell density, as measured by the $OD_{600,}$ was 1.20. (*B*) Outer membrane disruption of *E. coli* by MSI-78 and MSI-594: the blue shift in the fluorescence emission maximum indicates the extent of penetration of ANS into *E. coli* membrane as a function of peptide concentration.

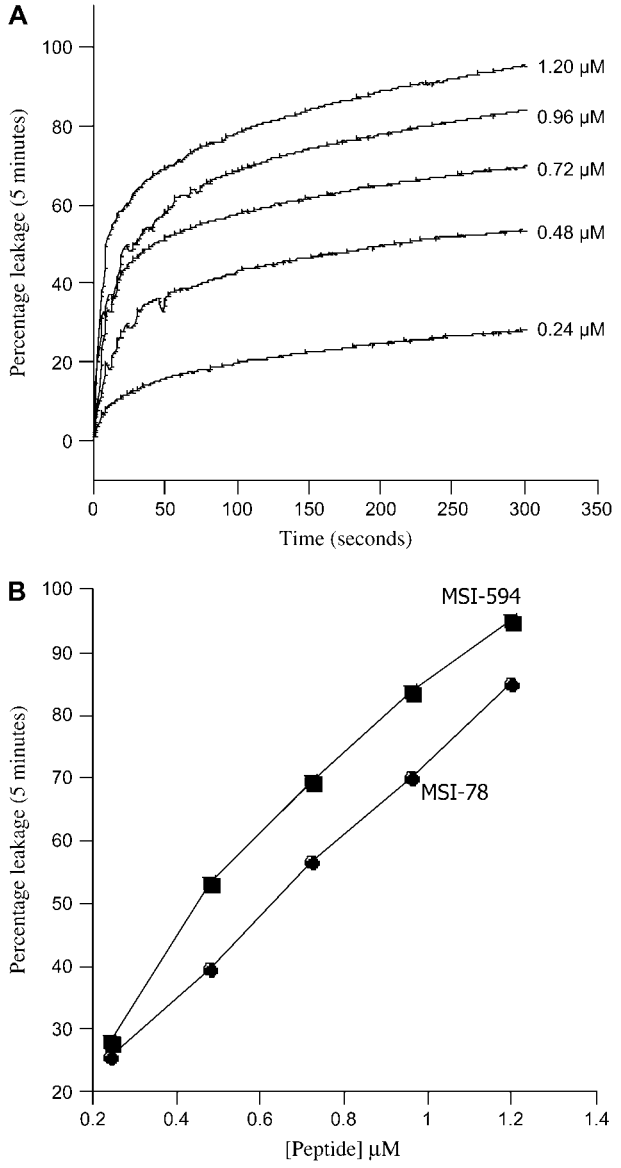

FIGURE 3 (*A*) Dye leakage profiles of MSI-594 from POPC-POPG (3:1) SUVs. Lipid concentration was 80 μM. (*B*) Relative efficacies of MSI-78 and MSI-594 to induce dye leakage from POPC/POPG (3:1) SUVs. Percentage dye leakage in 5 min is plotted against the concentration of the peptides.

bilayers for 1 or 3 mol % MSI-78. Since the peptide forms a helical structure in lipid bilayers, these data can be interpreted in terms of the orientation of the peptide in bilayers. Based on the reported structural studies on the membrane-associated peptides using solid-state NMR (34–39), these data reveal that the helical MSI-78 is oriented on the bilayer surface (or perpendicular to the bilayer normal). A 2D PISEMA (40–43) experiment that correlates the ^{15}N chemical shift and the ^{1}H-^{15}N dipolar coupling was performed on the mechanically aligned bilayer sample. The PISEMA spectrum (Fig. 5 *B*) shows a dipolar splitting of 8.1 kHz. Based on the 2D PISEMA spectrum of an unaligned peptide that contains an amide-^{15}N label, a dipolar splitting of ~8 kHz corresponds to an orthogonal orientation of the N-H bond relative to the external magnetic field (42). Therefore, this data further confirms that MSI-78 is oriented with its helical axis perpendicular to the bilayer normal. The orientation of the helix slightly changes

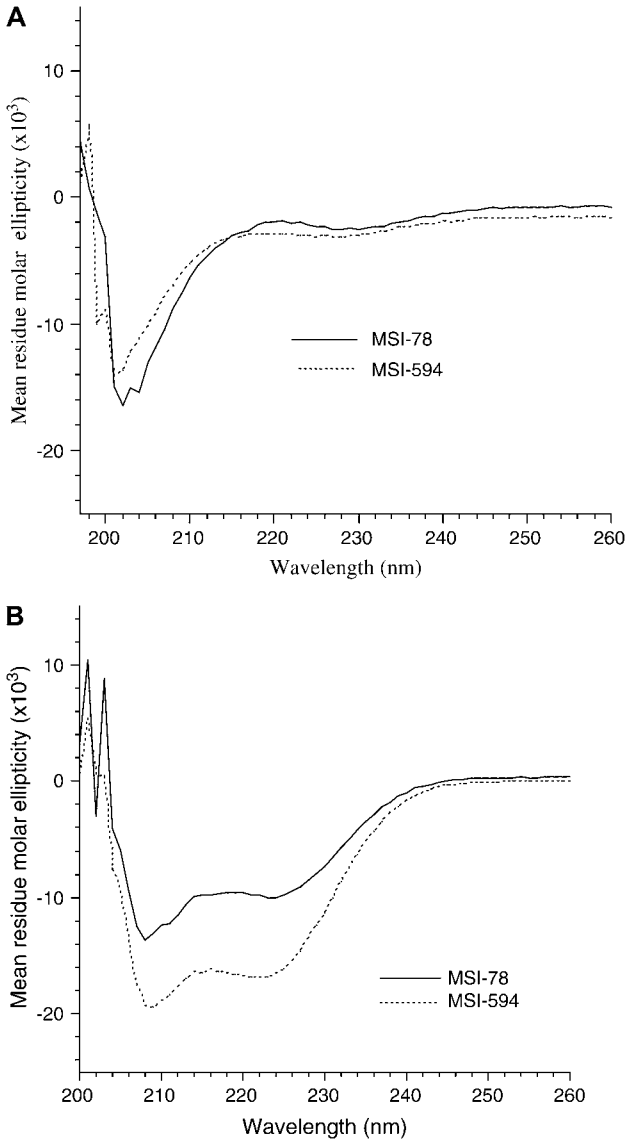

FIGURE 4 CD spectra of MSI-78 and MSI-594 in (*A*) Tris-buffer (10 mM Tris-HCl, 100 mM NaCl, 2 mM EDTA, pH 7.4) and (*B*) 2 mM POPC in Tris buffer. Peptide concentration was 20 μM and P/L was 1:100.

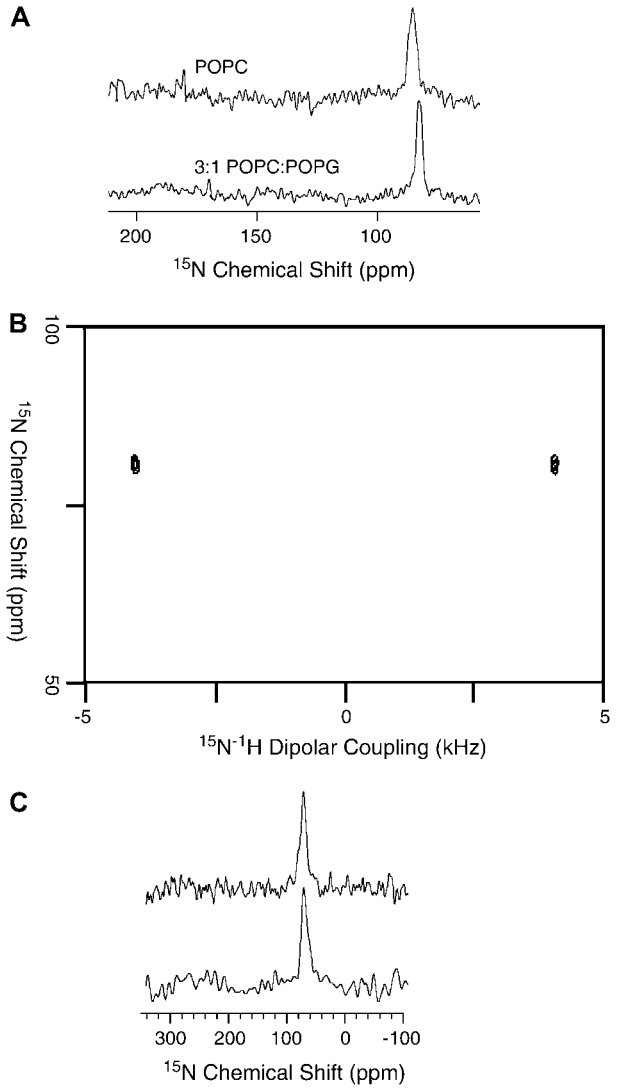

FIGURE 5 ^{15}N chemical shift spectra of mechanically aligned POPC (*top*) and 3:1 POPC/POPG (*bottom*) bilayers containing 3 mol % peptide: (*A*) MSI-78 and (*C*) MSI-594; 2,000 scans were used to obtain the spectra. (*B*) Two-dimensional PISEMA spectra of 3:1 POPC/POPG bilayers containing 3 mol % MSI-78 obtained using 48 t_1 experiments, 1500 scans, and a 2.5-s recycle delay.

with the bilayer composition. The presence of an anionic lipid POPG could enhance the lipid-peptide interaction and that would lead to a reduction in the heterogeneity of the peptide orientation in 3:1 POPC:POPG bilayers as compared to POPC bilayers. The ^{15}N chemical shift spectra of ^{15}N-Val$_{16}$-MSI-594 embedded in mechanically aligned POPC and 3:1 POPC/POPG bilayers are given in Fig. 5 *C*. A single chemical shift peak of ~76 ppm suggests an in-plane orientation of the helical MSI-594 in both the bilayers.

Interaction with lipid headgroups

To study the interaction of peptides with the lipid headgroup, ^{31}P NMR spectra were obtained from POPC and POPG bilayers incorporated with various concentrations of MSI-78 and MSI-594, and are presented in Figs. 6 and 7, respectively. In the absence of peptides, the lipid molecules are well oriented, as evidenced by the narrow symmetric line shape at ~30 ppm arising from the 0° (or parallel) orientation of lipids in bilayers. As demonstrated in our previous studies, samples prepared using the naphthalene procedure are well hydrated and stable (54); and therefore the signal appearing from the unoriented lipids (POPC in Fig. 6 and POPG in Fig. 7) is negligible. The incorporation of MSI-78 or MSI-594 into lipid bilayers results in asymmetric line shapes and also additional peaks at lower frequencies. For example, the incorporation of 1–5 mol % MSI-78 into POPC bilayers

TABLE 3 ^{15}N chemical shift (relative liquid ammonia) data obtained from experiments on aligned lipid bilayers with the bilayer normal parallel to the magnetic field direction

Peptide	Bilayers	^{15}N chemical shift (ppm)
1 mol % MSI-78	POPC	86 ± 3
3 mol % MSI-78	POPC	86 ± 3
5 mol % MSI-78	POPC	84 ± 4
7 mol % MSI-78	POPC	84 ± 4
1 mol % MSI-78	3:1 POPC:POPG	81 ± 1.5
3 mol % MSI-78	3:1 POPC:POPG	81 ± 1.5
5 mol % MSI-78	3:1 POPC:POPG	79 ± 3
7 mol % MSI-78	3:1 POPC:POPG	80 ± 3.5
1 mol % MSI-594	POPC	76 ± 3.5
3 mol % MSI-594	POPC	76 ± 4
5 mol % MSI-594	POPC	75 ± 4
7 mol % MSI-594	POPC	75 ± 4
1 mol % MSI-594	3:1 POPC:POPG	76 ± 4
3 mol % MSI-594	3:1 POPC:POPG	76 ± 4.5
5 mol % MSI-594	3:1 POPC:POPG	73 ± 3.5
7 mol % MSI-594	3:1 POPC:POPG	74 ± 4

results in the appearance of a low-intensity broad component that extends between 28 ppm and –18 ppm, suggesting the presence of lipids with different orientational distributions (Fig. 6). On the other hand, a high concentration of the MSI-78 peptide (15 mol %) in POPC bilayers results in a major peak at 5 ppm with a low-intensity signal appearing in the region 30 to −20 ppm. Although the presence of a lower concentration of MSI-594 (up to 5 mol %) does not induce a major change in the lamellar-phase POPC spectrum, at a higher concentration (15 mol %) of the peptide, the spectrum

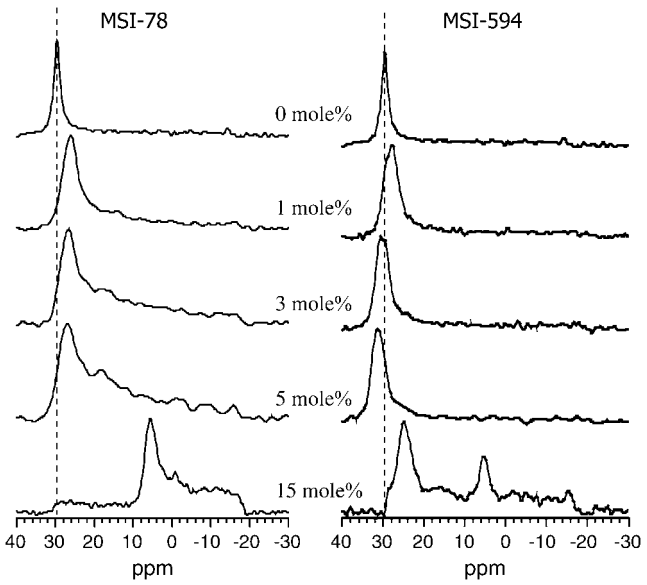

FIGURE 6 ^{31}P chemical shift spectra of aligned POPC bilayers in the presence and absence of MSI-78 and MSI-594. The peptide concentrations are indicated in the figure. Each spectrum was obtained from 2 mg lipids and required 100–1000 transients. Dashed line shows the frequency of the parallel edge of the pure POPC spectrum.

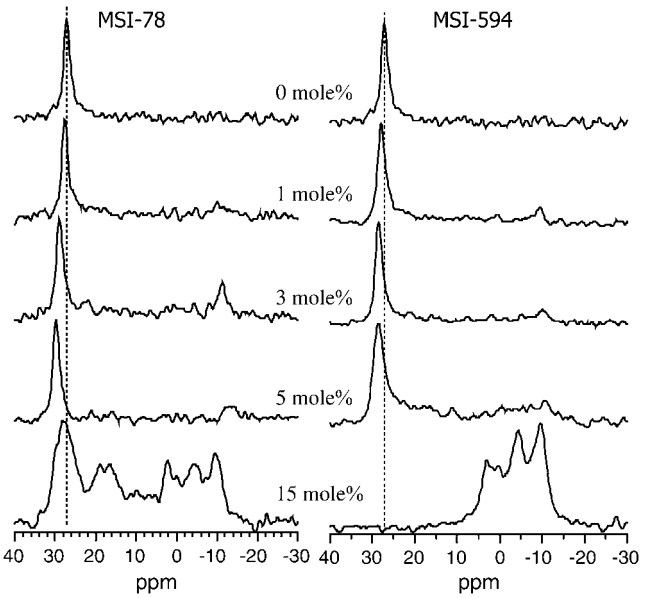

FIGURE 7 ^{31}P chemical shift spectra of aligned POPG bilayers in the presence and absence of MSI-78 and MSI-594. The peptide concentrations are indicated in the figure. Each spectrum was obtained from 2 mg lipids and required 100–1000 transients. Dashed line shows the frequency of the parallel edge of the pure POPG spectrum.

consists of peaks at 26 and 5 ppm (Fig. 6). The interaction of MSI-78 and MSI-594 with negatively charged POPG lipids is somewhat different (Fig. 7). The symmetric line shape observed from oriented POPG bilayers is slightly shifted downfield in the presence of up to 5 mol % of MSI-78 and MSI-594. Incorporation of 15 mol % MSI-78 results in several asymmetrical ^{31}P-NMR line shapes in the range from 22 ppm to −18 ppm, with the major component appearing at ~29 ppm. However, the addition of 15 mol % MSI-594 completely abolishes the oriented POPG component at ~28 ppm and yields broad asymmetric peaks in the range from 5 ppm to −10 ppm (Fig. 7), indicating that a high concentration of peptides induce the formation of nonbilayer structures. These results are discussed below.

Influence on the lipid acyl chains

Since the binding of peptides at the membrane interface could affect the acyl chain dynamics of lipid bilayers, ^{2}H NMR spectra were collected from peptide-containing POPC-d_{31} MLVs to assess the disorder in the lipid acyl chain. Fig. 8 *A* shows the de-Paked ^{2}H NMR spectra of pure and peptide containing (P/L ratio 1:33) POPC-d_{31} dispersions. In the absence of peptide, POPC-d_{31} bilayers display resolved quadrupolar couplings in the range 5.5–51.0 kHz. The order parameters derived from these quadrupolar splittings characterize the varying dynamic order of methylene groups along the lipid acyl chain (29,30,44–46). The ^{2}H NMR spectra of POPC-d_{31} MLVs containing 3 mol % MSI-78 or

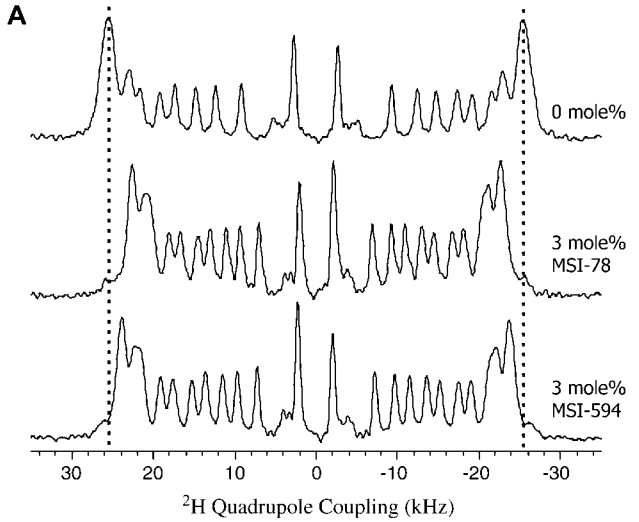

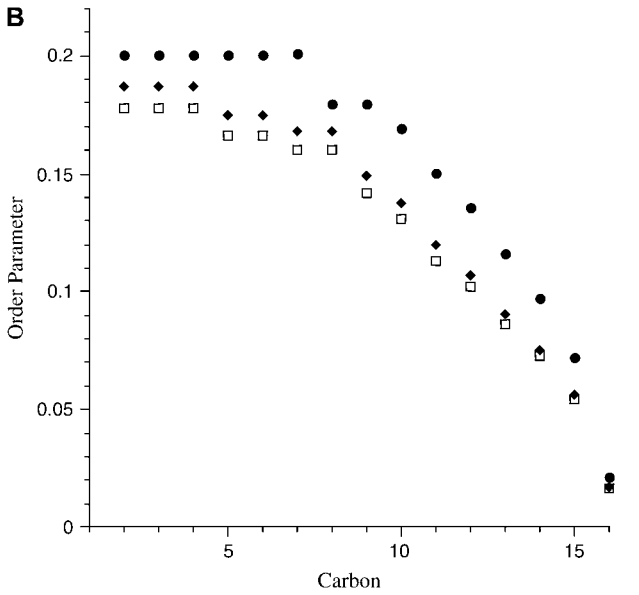

FIGURE 8 (*A*) de-Paked ^{2}H quadrupole coupling spectra of POPC-d_{31} MLVs and POPC-d_{31} MLVs incorporated with 3 mol % MSI-78 and MSI-594. (*B*) Plot of order parameter versus lipid acyl chain carbon number: POPC-d_{31} (●), POPC-d_{31}/MSI-78 (□), and POPC-d_{31}/MSI-594 (♦).

MSI-594 exhibit a reduction in the quadrupolar splitting while maintaining the line shape characteristic of the fluid L_α phase of POPC. This corresponds to a decrease in the acyl chain order parameters as shown in Fig. 8 *B*.

Curvature strain determined using DSC

Membrane binding of antimicrobial peptides can induce negative or positive curvature strain depending on the nature of lipid-peptide interactions (47,48). Since MSI-78 and MSI-594 bind to the surface of lipid bilayers, the L_α-to- H_{II} phase transition temperature of DiPoPE bilayers in the presence of MSI-78 or MSI-594 was measured to assess the curvature strain exerted on the membrane. The representative DSC thermograms of DiPoPE MLVs incorporated with various amounts of MSI-78 or MSI-594 are presented in Fig. 9. Pure DiPoPE MLVs displayed L_α to H_{II} phase transition at 43°C, which is consistent with the value reported in the literature (49). However, DiPoPE MLVs incorporated with 0.4 mol % MSI-78 and 0.4 mol % MSI-594 exhibited phase transitions at 46°C and 47°C, respectively. The increase in phase transition temperature suggests that both MSI-78 and MSI-594 repress the lamellar-to-inverted hexagonal phase transition of DiPoPE vesicles by inducing positive curvature strain on bilayers.

DISCUSSION

The outer membrane of Gram-negative bacteria acts as a barrier to drugs. As such, one of the initial steps of drug activity is outer membrane disruption (49). MSI-78 and MSI-594 exhibit potent activity against both Gram-positive and Gram-negative bacteria and are significantly more active than magainin 2 (Table 2). Therefore, it is necessary to ascertain the effective concentrations of MSI-78 and MSI-594 needed for outer membrane permeabilization so as to assess the relation between outer membrane disruption and the antibiotic susceptibility. As shown in Fig. 2, both the peptides perturbed the outer membrane of *E. coli* (cell density

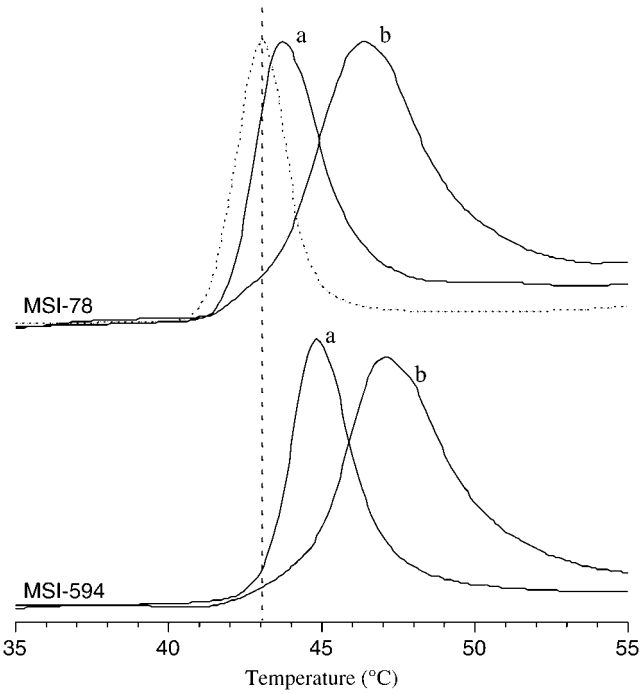

FIGURE 9 DSC thermograms of DiPoPE incorporated with different concentrations of MSI-78 and MSI-594. The heating scan rate was 1°C/min. The vertical dotted line shows the phase transition temperature ($T_m = 43$°C) of pure DiPoPE (*dotted line*). The phase transition of DiPoPE containing 0.2 mol % (*a*) and 0.4 mol % (*b*) peptide are shown by solid lines.

$A_{600} = 1.20$) at concentrations that were much lower than their MIC (cell density $A_{600} = 0.02$) values. The low concentrations needed for outer membrane disruption suggest that other factors are involved in the bacterial killing process. The maximum blue shift in the emission maximum of ANS observed for MSI-78 (Fig. 2 *B*) can be attributed to a higher degree of disruption of the outer membrane. MSI-594 is more hydrophobic, more helical, and less cationic than MSI-78. The degree of outer membrane disruption induced by MSI-594 is less than that induced by MSI-78 (Fig. 2 *B*). However, both MSI-594 and MSI-78 exhibit antimicrobial activities at comparable concentrations (Table 2). This suggests that outer membrane disruption per se is not sufficient for antimicrobial activity. The inner membrane of Gram-negative bacteria contains PE (65%), PG (15%), cardiolipin (15%), and other lipids (15%), and therefore is negatively charged. We used negatively charged SUVs composed of POPC/POPG (3:1) lipids to assess the ability of the peptides to permeabilize bacterial inner membrane. As shown in Fig. 3, both MSI-594 and MSI-78 cause the leakage of carboxyfluorescein dye from POPC/POPG (3:1) vesicles at comparable concentrations. Since the concentrations of MSI-78 and MSI-594 needed to kill bacteria (MIC values) and permeabilize the negatively charged membrane are comparable, permeabilization of bacterial inner membrane seems to be critical for the observed antimicrobial activity. Our observation is consistent with the earlier report on magainin (50).

It has been shown in the case of magainin 2 that the helix formation dominates the binding enthalpy and acts as a driving force for membrane binding (50). Since membrane permeabilization is coupled with helix formation, we examined the structure of MSI-78 and MSI-594 in aqueous medium and zwitterionic lipid membrane. Both MSI-78 and MSI-594 show an unordered structure in aqueous medium (Fig. 4 *A*). However, they adopt α-helical conformation upon binding to lipid vesicles (Fig. 4 *B*). The ^{15}N NMR data given in Fig. 5 suggest that the amphipathic helical peptides are oriented on the bilayer surface, nearly perpendicular to the bilayer normal. Although this observation is similar to other naturally occurring magainin peptides, a recent NMR study showed that the orientation of PGLa in lipid bilayers depends on the concentration of the peptide (51). On the other hand, ^{15}N experiments performed on 3:1 POPC/POPG bilayers containing 5 and 7 mol % of peptides did not show a significant change in the ^{15}N chemical shift peak position (Table 3). These data suggest that the orientation of MSI-78 and MSI-594 are similar within experimental errors and that the peptides do not have a transmembrane orientation. Further studies are required to understand the three-dimensional structure of the peptide in monomeric or oligomeric forms. Therefore, it is most likely that these peptides do not function via the barrel-stave mechanism of membrane disruption. An empirical estimate of the amount of secondary structure shows 34% and 57% helical contents for MSI-78 and MSI-594, respectively. Considering the comparable antimicrobial properties of MSI-78 and MSI-594, there seems to be no direct correlation between helicity and antimicrobial activity.

Because antimicrobial peptides target the physicochemical properties of lipid membranes, ^{31}P and ^{2}H NMR methods were used to study the lipid-peptide interactions. Though MIC values for MSI-78 and MSI-594 have been measured in bulk solution, the exact concentration of the peptide on the membrane surface is not known. High concentrations of the peptides were used in solid-state NMR experiments to mimic the high concentrations of peptides likely to be present on the cell membrane surface and pore complexes. Lipids in pure POPC bilayers remain well aligned and give a symmetric peak at ~30 ppm (Fig. 6). The incorporation of 1–5 mol % MSI-78 in POPC bilayers results in lipids with different orientational distributions, which is consistent with a toroidal-type complex formation, as discussed in our previous study (52). However, the incorporation of 15 mol % MSI-78 induces a major peak at ~5 ppm (Fig. 6) that may be due to the formation of hexagonal-type lipid structures (22). MSI-594 shows a similar effect on POPC bilayers albeit with a lesser magnitude (Fig. 6 *B*). Since these peptides induce positive curvature strain on bilayers (Fig. 9), it is likely that these lipid structures are normal-hexagonal rather than inverted-hexagonal phase structures. As this observation was made at a very high peptide concentration and may not be relevant to understanding the biological function of the peptide, more experiments are needed to understand the structure of lipids in detail. These results suggest that the mechanisms of POPC bilayer disruption by these two peptides differ: whereas MSI-78 appears to induce toroidal-type distribution of lipid orientations, MSI-594 could function via a carpet mechanism. The carpet mechanism of membrane distribution is in agreement with several studies on linear peptides (8,39,46,53).

The effect of MSI-78 in POPG bilayers differs from that in POPC bilayers. The incorporation of 15 mol % MSI-78 in POPG bilayers induces the formation of nonbilayer lipid phases (Fig. 7). It may also be possible that a lack of bulk water in mechanically aligned bilayers could lead to the formation of nonlamellar phases in the sample. However, such nonlamellar phases were not observed in the absence of the peptide, nor were they observed for other antimicrobial peptides we have studied (54,55). These results are further confirmed by the mechanical rotation of the sample, as discussed in our previous study on MSI-78 (22). MSI-594 also interacts differently with POPC and POPG bilayers. The incorporation of 15 mol % MSI-594 with POPG results in nonbilayer structures including the H_I-type phase as evidenced by the peak at ~5 ppm (Fig. 7). POPG bilayers containing up to 5 mol % MSI-594 show that the majority of the lipids are aligned along the magnetic field and the remaining lipids are slightly disordered. Such lipid-peptide interactions would also lead to a reduction in the lipid acyl chain order. The acyl chain order parameters derived from POPC MLVs incorporated with 3 mol % MSI-78 or

MSI-594, show a general disorder at the methylene units near the glycerol backbone and the effect gradually decreases along the chain toward the other end (Fig. 8). These results are consistent with the recent AFM study that showed MSI-78-induced bilayer thinning, whereas solid-state NMR experiments showed the MSI-78-induced disorder in dimyristoylphosphatidylcholine bilayers (23).

The positive curvature strain is known to facilitate the formation of toroidal pores in the case of magainin 2 (48). In the case of MSI-78 and MSI-594, the lipid-peptide interactions leading to the disorder in the headgroup and acyl chain regions and a domain of H_I-type lipid structure are most likely the result of peptide-induced positive curvature strain on lipid bilayers. This assumption is consistent with our observation from DSC experiments (Fig. 9). The L_α-to-H_{II} phase transition temperature of DiPoPE MLVs increases from 43°C to 45°C and 46°C when 0.4 mol % MSI-78 and 0.4 mol % MSI-594 are incorporated. It appears from the DSC data that MSI-78 and MSI-594 stabilize the L_α phase at higher temperatures by imposing positive curvature strain in lipid bilayers. Similar results were obtained from ^{31}P NMR experiments on POPE bilayers (data not shown). A similar observation was also made in the case of LL37-incorporated bilayers composed of the *E. coli* total lipid extract, in which POPE is the major component (55).

CONCLUSION

We have investigated the mechanism of membrane interaction of two amphipathic antimicrobial peptides, MSI-78 and MSI-594, derived from magainin 2 and melittin. Both the peptides show excellent antimicrobial activity and adopt α-helical conformation upon binding to membrane. There is no direct correlation between helical content and antimicrobial activity. *E.coli* outer membrane disrupting ability correlates with the cationicity of the peptides. Permeabilization of negatively charged membrane mimicking bacterial inner membrane and antimicrobial activity are observed at comparable concentrations. Solid-state NMR results reveal that the peptides are oriented nearly parallel to the bilayer surface, and suggest that it is most likely that these peptides do not function via the barrel-stave membrane-disruption mechanism. On the other hand, DSC and ^{31}P NMR results suggest that the incorporation of peptides into lipid bilayers imparts positive curvature strain and results in disorder in the headgroup as well as in the acyl chain region of lipids. In addition, ^{31}P data suggest that the peptide-induced disorder depends on the lipid composition of bilayers. Taken together, our data account for a carpet mechanism of membrane disruption for MSI-594, whereas MSI-78 functions via carpet mechanism in POPG bilayers and via toroidal-type mechanism in POPC bilayers.

We thank Dr. Kevin Hallock and Dr. Henzler-Wildman for helpful discussions.

This research was supported by funds from the National Instistiutes of Health (AI054515).

REFERENCES

1. Zasloff, M. 2002. Antimicrobial peptides of multicellular organisms. *Nature*. 415:389–395.
2. Boman, H. G. 1995. Peptide antibiotics and their role in innate immunity. *Annu. Rev. Immunol.* 13:61–92.
3. Shai, Y. 2002. From innate immunity to *de-novo* designed antimicrobial peptides. *Curr. Pharm. Des*. 8:715–725.
4. Wade, D., A. Boman, B. Wahlin, C. M. Drain, D. Andreu, H. G. Boman, and R. B. Merrifield. 1990. All-D amino acid-containing channel-forming antibiotic peptides. *Proc. Natl. Acad. Sci. USA*. 87:4761–4765.
5. Bessalle, R., A. Kapitkovsky, A. Gorea, I. Shalit, and M. Fridkin. 1990. All-D-magainin: chirality, antimicrobial activity and proteolytic resistance. *FEBS Lett*. 274:151–155.
6. Matsuzaki, K. 1998. Magainins as paradigm for the mode of action of pore forming polypeptides. *Biochim. Biophys. Acta*. 1376:391–400.
7. Ladokhin, A. S., M. E. Selsted, and S. H. White. 1997. Sizing membrane pores in lipid vesicles by leakage of co-encapsulated markers: pore formation by melittin. *Biophys. J*. 72:1762–1766.
8. Shai, Y. 1999. Mechanism of the binding, insertion and destabilization of phospholipid bilayer membranes by α-helical antimicrobial and cell non-selective membrane-lytic peptides. *Biochim. Biophys. Acta*. 1462: 55–70.
9. Dathe, M., M. Schumann, T. Wieprecht, A. Winkler, K. Matsuzaki, O. Murase, M. Beyermann, E. Krause, and M. Bienert. 1996. Peptide helicity and membrane surface charge modulate the balance of electrostatic and hydrophobic interactions with lipid bilayers and biological membranes. *Biochemistry*. 35:12612–12622.
10. Ladokhin, A. S., and S. H. White. 2001. Detergent-like'' permeabilization of anionic lipid vesicles by melittin. *Biochim. Biophys. Acta*. 1514: 253–260.
11. Hawkey, P. M. 1998. The origins and molecular basis of antibiotic resistance. *BMJ*. 317:657–660.
12. Hancock, R. E. W. 2003. Concerns regarding resistance to self-proteins. *Microbiology*. 149:3343–3344.
13. Maloy, W. L., and U. P. Kari. 1995. Structure-activity studies on magainins and other host defense peptides. *Biopolymers*. 37:105–122.
14. Epand, R. F., L. Raguse, S. H. Gellman, and R. M. Epand. 2004. Antimicrobial 14-helical β-peptides: potent bilayer disrupting agents. *Biochemistry*. 43:9527–9535.
15. Wieprecht, T., M. Dathe, and E. Krause. 1997. Modulation of membrane activity of amphipathic, antibacterial peptides by slight modifications of the hydrophobic moment. *FEBS Lett*. 417:135–140.
16. Matsuzaki, K., K. Sugishita, N. Fujii, and K. Miyajima. 1995. Molecular basis for membrane selectivity of an antimicrobial peptide, magainin 2. *Biochemistry*. 34:3423–3429.
17. Dathe, M., M. Schumann, T. Wieprecht, A. Winkler, M. Beyermann, E. Krause, K. Matsuzaki, O. Murase, and M. Bienert. 1996. Peptide helicity and membrane surface charge modulate the balance of electrostatic and hydrophobic interactions with lipid bilayers and biological membranes. *Biochemistry*. 35:12612–12622.
18. Uematsu, N., and K. Matsuzaki. 2000. Polar angle as a determinant of amphipathic α-helix-lipid interactions: a model peptide study. *Biophys. J*. 79:2075–2083.
19. Cornut, I., K. Buttner, J.-L. Dasseux, and J. Dufourcq. 1994. The amphipathic α-helix concept: application to the de novo design of ideally amphipathic Leu, Lys peptides with hemolytic activity higher than that of melittin. *FEBS Lett*. 349:29–33.
20. Zasloff, M., B. Martin, and H.-C. Chen. 1998. Antimicrobial activity of synthetic magainin peptides and several analogues. *Proc. Natl. Acad. Sci. USA*. 85:910–913.

21. Dempsey, C. E. 1990. The actions of melittin on membranes. *Biochim. Biophys. Acta.* 31:143–161.

22. Hallock, K. J., D. K. Lee, and A. Ramamoorthy. 2003. MSI-78, an analogue of the magainin antimicrobial peptides, disrupts lipid bilayer structure via positive curvature strain. *Biophys. J.* 84:3052–3060.

23. Mecke, A., D. K. Lee, A. Ramamoorthy, B. Orr, and M. Banaszak Holl. 2005. Membrane thinning due to antimicrobial peptide binding: an atomic force microscopy study of MSI-78 in lipid bilayers. *Biophys. J.* 99:4043–4050.

24. Thennarasu, S., D. K. Lee, A. Tan, U. Prasad Kari, and A. Ramamoorthy. 2005. Antimicrobial activity and membrane selective interactions of a synthetic lipopeptide MSI-843. *Biochim. Biophys. Acta.* 1711:49–58.

25. Rohl, C. A., and R. L. Baldwin. 1997. Comparison of NH exchange and circular dichroism as techniques for measuring the parameters of the helix-coil transition in peptides. *Biochemistry.* 36:8435–8442.

26. Hallock, K. J., K. H. Wilderman, D. K. Lee, and A. Ramamoorthy. 2002. An innovative procedure using a sublimable solid to align lipid bilayers for solid-state NMR studies. *Biophys. J.* 82:2499–2503.

27. Washburn, E. W., C. J. West, and C. Hull. 1926. International Critical Tables of Numerical Data, Physics, Chemistry, and Technology. McGraw-Hill, New York.

28. Sternin, E., M. Bloom, and A. L. MacKay. 1983. De-Pake-ing of NMR spectra. *J. Magn. Reson.* 55:274–282.

29. Sternin, E., B. Fine, M. Bloom, C. P. S. Tilcock, K. F. Wong, and P. R. Cullis. 1988. Acyl chain orientational order in the hexagonal H_{II} phase of phospholipid-water dispersions. *Biophys. J.* 54:689–694.

30. Seelig, J., and H.-U. Gally. 1976. Investigation of phosphatidylethanolamine bilayers by deuterium and phosphorus-31 nuclear magnetic resonance. *Biochemistry.* 15:5199–5204.

31. Fauchere, J.-L., and V. Pliska. 1983. Hydrophobic parameters of amino acid-side chains from the partioning of N-acetyl-amino-acid amides *Eur. J. Med. Chem.-. Chim. Ther.* 18:369–375.

32. Eisenberg, D., E. Schwarz, M. Komarony, and R. Wall. 1984. Analysis of membrane and surface protein sequences with the hydrophobic moment plot. *J. Mol. Biol.* 179:125–142.

33. Beschiaschvili, G., and J. Seelig. 1990. Melittin binding to mixed phosphatidylglycerol/phosphatidylcholine membranes. *Biochemistry.* 29: 52–58.

34. Ramamoorthy, A., F. Marassi, M. Zasloff, and S. J. Opella. 1995. Three-dimensional solid-state NMR spectroscopy of a peptide oriented in membrane bilayers. *J. Biomol. NMR.* 6:329–334.

35. Marassi, F. M., A. Ramamoorthy, and S. J. Opella. 1997. Complete resolution of the solid-state NMR spectrum of a uniformly ^{15}N-labeled membrane protein in phospholipid bilayers. *Proc. Natl. Acad. Sci. USA.* 94:8551–8556.

36. Lee, D. K., J. S. Santos, and A. Ramamoorthy. 1999. Application of one-dimentional dipolar shift solid-state NMR spectroscopy to study the back bone conformation of membrane-associated peptides in phospholipid bilayers. *J. Phys. Chem.* B103:8383–8390.

37. Marassi, F. M., and S. J. Opella. 2000. A solid-state NMR index of helical membrane protein structure and topology. *J. Magn. Reson.* 144: 150–155.

38. Wang, J., J. Denny, C. Tian, S. Kim, Y. Mo, F. Kovacs, Z. Song, K. Nishimura, Z. Gan, R. Fu, J. R. Quine, and T. A. Cross. 2000. Imaging membrane protein helical wheels. *J. Magn. Reson.* 144:162–167.

39. Strandberg, E., and A. S. Ulrich. 2004. NMR methods for studying membrane-active antimicrobial peptides. *Concept. Magn. Reson.* 23A: 89–120.

40. Wu, C. H., A. Ramamoorthy, and S. J. Opella. 1994. High resolution heteronuclear dipolar solid-state NMR spectroscopy. *J. Magn. Reson.* A109:270–272.

41. Ramamoorthy, A., C. H. Wu, and S. J. Opella. 1999. Experimental aspects of multidimensional solid-state NMR correlation spectroscopy. *J. Magn. Reson.* 140:131–140.

42. Ramamoorthy, A., Y. Wei, and D. K. Lee. 2004. PISEMA solid-state NMR spectroscopy. *Annu. Rep. NMR Spectrosc.* 52:1–52.

43. Yamamoto, K., D. K. Lee, and A. Ramamoorthy. 2005. Broadband-PISEMA solid-state NMR spectroscopy. *Chem. Phys. Lett.* 407: 289–293.

44. Wildman, K. H., G. V. Martinez, M. F. Brown, and A. Ramamoorthy. 2004. Perturbation of the hydrophobic core of lipid bilayers by the human antimicrobial peptide LL-37. *Biochemistry.* 43:8459–8469.

45. Porcelli, F., B. Buck, D. K. Lee, K. J. Hallock, A. Ramamoorthy, and G. Veglia. 2004. Structure and orientation of pardaxin determined by NMR experiments in model membranes. *J. Biol. Chem.* 279:46815–46823.

46. Lu, J. X., K. Damodaran, J. Blazyk, and G. A. Lorigan. 2005. Solid-state nuclear magnetic resonance relaxation studies of the interaction mechanism of antimicrobial peptides with phospholipid bilayer membranes. *Biochemistry.* 44:10208–10217.

47. Wieprecht, T., M. Dathe, R. M. Epand, M. Beyermann, E. Krause, W. L. Maloy, D. L. MacDonald, and M. Bienert. 1997. Influence of the angle subtended by the positively charged helix face on the membrane activity of amphipathic, antimicrobial peptides. *Biochemistry.* 36:12869–12880.

48. Matsuzaki, K., K. Sugishita, N. Ishibe, M. Ueha, S. Nakata, M. Miyajima, and R. M. Epand. 1998. Relationship of membrane curvature to the formation of pores by magainin 2. *Biochemistry.* 37:11856–11863.

49. Hancock, R. E. W. 1997. The bacterial outer membrane as a drug barrier. *Trends Microbiol.* 5:37–42.

50. Wu, M., E. Maier, R. Benz, and R. E. W. Hancock. 1999. Mechanism of interaction of different classes of cationic antimicrobial peptides with planar bilayers and with the cytoplasmic membrane of *Escherichia coli*. *Biochemistry.* 38:7235–7242.

51. Glaser, R. W., C. Sachse, U. H. N. Dürr, P. Wadhwani, S. Afonin, E. Strandberg, and A. S. Ulrich. 2005. Concentration-dependent realignment of the antimicrobial peptide PGLa in lipid membranes observed by solid-state ^{19}F-NMR. *Biophys. J.* 88:3392–3397.

52. Matsuzaki, K., O. Murase, N. Fujii, and K. Miyajima. 1996. An antimicrobial peptide, magainin 2, induced rapid flip-flop of phospholipids coupled with pore formation and peptide translocation. *Biochemistry.* 35:11361–11368.

53. Toke, O., W. L. Maloy, S. J. Kim, J. Blazyk, and J. Schaefer. 2004. Secondary structure and lipid contact of a peptide antibiotic in phospholipid bilayers by REDOR. *Biophys. J.* 87:662–674.

54. Hallock, K. J., D. K. Lee, J. Omnaas, H. I. Mosberg, and A. Ramamoorthy. 2002. Membrane composition determines pardaxin's mechanism of lipid bilayer disruption. *Biophys. J.* 83:1004–1013.

55. Wildman, K. A. H., D. K. Lee, and A. Ramamoorthy. 2003. Mechanism of lipid bilayer disruption by the human antimicrobial peptide, LL-37. *Biochemistry.* 42:6545–6558.